Synchronizing network systems in the presence of limited resources via edge snapping

Alessandra Corso,[1] Lucia Valentina Gambuzza,[1] Pietro De Lellis,[2] and Mattia Frasca[1]
[1)] *Department of Electrical Electronic and Computer Science Engineering, University of Catania, Catania, Italy.*
[2)] *Department of Electrical Engineering and Information Technology, University of Naples Federico II, Naples, Italy.*

(*Electronic mail: mattia.frasca@dieei.unict.it)
(Published version: https://doi.org/10.1063/5.0093560)

In this work, we propose a multilayer control protocol for synchronization of network dynamical systems under limited resources. In addition to the layer where the interactions of the system takes place, i.e., the backbone network, we propose a second, adaptive layer, where the edges are added or removed according to the edge snapping mechanism. Different from classic edge snapping, the inputs to the edge dynamics are modified to cap the number of edges that can be activated. After studying local stability of the overall network dynamics, we illustrate the effectiveness of the approach on a network of Rössler oscillators, and then show its robustness in a more general setting, exemplified with a model of the Italian high-voltage power grid.

In biology, adaptation describes the process that permits a structure to cope with changes to the environmental conditions. This concept has inspired a plethora of applications in artificial systems, including optimization algorithms and artificial intelligence. In the context of dynamical systems, adaptation allows to design controllers that are able to readjust the intensity and modalities of their inputs as a function of the system operating conditions. More specifically, adaptation has been used in networks of coupled dynamical systems to control synchronization, by incorporating updating mechanisms for the network describing the interactions between the units composing the system. Most of the works on this topic have considered models where the network evolution is not constrained. However, towards realistic applications, one should account for limitations on the available resources and, therefore, on the number of connections between the units in the system. A few researches have analyzed this problem, focusing on phase (Kuramoto) oscillators. Here, we study the more general case of networks with arbitrary dynamics incorporating an adaptive strategy that limits the number of connections each unit can have.

I. INTRODUCTION

Adaptive networks can be described as an ensemble of dynamical units coupled over a graph topology, whose structure coevolves with the dynamics taking place at each unit[1,2]. The idea of associating dynamics not only to the nodes but also to the edges of a network can be traced back to the pioneering work of Šiljak[3], who later formalized the concept of dynamic graphs[4]. The key feature of these graphs is that weights can dynamically evolve (with a dependence described by a differential equation) and adjust in response to some external driver. However, dynamic graphs do not incorporate any growth mechanism, which, instead, is taken into account in the Holland's notion of complex adaptive systems[5]. Both the adaptation and the growth mechanism in networks are framed into the more general framework of the *evolving dynamical networks*, where the network dynamics take place within the set of admissible generalized dynamic graphs, possibly having different size[6,7].

In the last decades, the descriptive power of adaptive networks has been used to represent, analyze, and control both natural and artificial systems. Indeed, many social and biological interacting systems possess the ability of reshaping the structure of interactions by forming or suppressing interconnections among their constituents and/or modulating their strength[8], and therefore can be readily described as adaptive networks[9]. Inspired by natural systems, adaptive networks have also been employed to design control mechanisms for artificial systems, whereby tuning the weight of a link or rewiring the structure of the interactions facilitates the achievement of a desired collective behavior for the network system[7]. In particular, synchronization, i.e., the process through which interacting oscillators converge to a common trajectory, is a collective behavior that is often targeted in adaptive networks[10].

Adaptation may be incorporated in a network in different ways. In a first bulk of work, the network structure is assumed constant, whereas the weights of the edges are adapted to foster network synchronization. First, centralized adaptation strategies have been proposed, framing for all network links the same weight updated simultaneously with a law that depends on global information on the state of all nodes[11,12]. An alternative decentralized approach, which does not require a global information exchange between all the network nodes, prescribes that each node dynamically negotiates with its neighbors the intensity of their mutual coupling, depending on the mismatch between their states, so that an adaptive coupling is associated to each node or link in the network[10,12].

Later work then considered that not only the edge weights can be modulated, but also the network structure itself can be dynamically updated, with connections added or removed toward synchronizing the dynamics taking place at each node[7,13]. This approach has been, for instance, pursued in coupled Kuramoto oscillators, showing the emergence of structures at meso- and macro-scales[14,15]. Notably, the adap-

tive laws proposed in these works incorporate constraints on the overall intensity of the coupling. For more general individual dynamics, possibly exhibiting chaotic oscillations, the so-called edge snapping mechanisms was proposed to describe the activation or deactivation of a given edge, whose state evolution was described as that of a mass in a double-well potential, driven by the mismatch between the states of its endpoints[7]. The presence of inertia in the edge dynamics implies that an edge is only activated if this mismatch is sufficiently high and persistent, thereby preventing the activation of edges due to temporary, short perturbations.

The edge snapping mechanism was successfully employed to describe the dynamics that lead to the emergence of a steady-state topology in complex networks. Interestingly, when applied to capture the influence dynamics in financial networks, the emerging degree distribution reproduced that observed in corporate elite networks[16,17]. From a control perspective, edge snapping can also be viewed as a control mechanism, where the network topology continues to evolve until synchronization or pinning control is achieved[7,18]. Nonetheless, towards its application in technological contexts, it is necessary to consider the presence of possible limitation of the available resources, which prevent the activation of an excessive number of edges. Indeed, depending on the initial conditions, networks with large steady-state average degree may emerge[19].

In this paper, we propose to overcome this problem for a general complex network model, whereby we modify the edge snapping dynamics to explicitly account for constraints on the number of activated edges. Towards this aim, we adopt a multilayer framework as in Ref.[20,21]. In this general framework, a layer represents the physical system to control, while the others implement the different functionalities of the control law, such as, for instance, the modes of a distributed proportional, integral and derivative controller. Synchronization in multilayer networks has been also studied in the case where, instead, the layers represent different types of interactions existing in the physical system[22–25].

In more detail, here we consider that the system is composed by two layers. The first layer constitutes the (static) backbone network, whereas the second is a switching adaptive control layer that determines the additional edges to be activated. Different from classic edge snapping, here i) edges are activated or deactivated through a discontinuous output function of the edge state, and ii) the input to the snapping dynamics is designed to regulate the trade-off between the need of activating new edges to foster synchronization and that of avoiding activating an excessive number of edges. Indeed, the discontinuous, binary edge output function allows each node to independently count the number of incident activated edges, whereas the input to the edge dynamics allows to asymptotically constrain the degree of each node. We analytically show that, under suitable assumptions on the individual dynamics and coupling strength, locally asymptotically stable steady-state network configurations exist. Furthermore, we provide a lower bound on the coupling strength, below which the snapping dynamics cannot induce synchronization among the network nodes.

The effectiveness of the approach is demonstrated on networks of chaotic Rössler oscillators. Then, we aim at characterizing the robustness of the proposed modified edge snapping mechanism in a more general modeling setting. Toward this goal, we consider a model of the Italian high-voltage power grid, and test its ability of reacting to faults. In this context, we evaluate how the control layer is capable of reconfiguring following a fault at a given line.

II. MULTILAYER NETWORK MODEL

A. Node dynamics

Let us consider an undirected multilayer network composed by N systems, whose dynamics are given by

$$\begin{aligned}\dot{x}_i(t) = f(x_i) + k\sum_{j=1}^{N} a^b_{ij}(h^b(x_j(t)) - h^b(x_i(t))) \\ + q\sum_{j=1}^{N} a^c_{ij}(t)(h^c(x_j(t)) - h^c(x_i(t))), \quad i = 1,\dots,N,\end{aligned} \tag{1}$$

where $x_i \in \mathbb{R}^n$ is the state of the $i-$th node, and $f : \mathbb{R}^n \to \mathbb{R}^n$ is the vector field describing the individual dynamics. The interaction between the units takes place on two layers, a backbone layer describing the pre-existing connections between the units, and an additional control layer to be appropriately designed. The topology of the backbone layer is described by the backbone adjacency matrix, whose element a^b_{ij} is 1 if there is a backbone link between units i and j, whereas it is 0 otherwise; k is the strength of the coupling in the backbone layer, whereas $h^b : \mathbb{R}^n \to \mathbb{R}^n$ is the inner coupling function of the backbone layer. Similarly, the inner coupling of the control layer is described by $h^c : \mathbb{R}^n \to \mathbb{R}^n$, with a coupling strength given by the scalar q. Different from the backbone network, the topology of the control layer is time-varying, and is described by a time-varying adjacency matrix $A^c(t)$ whose element ij is denoted $a^c_{ij}(t)$, and is 1 if an edge of the control layer connects nodes i and j at time t, whereas it is 0 otherwise.

B. Design of the control layer topology

The scope of the control layer is to simultaneously reach the following, possibly contrasting goals

$$\lim_{t\to+\infty}(x_i(t) - x_j(t)) = 0, \quad i,j = 1,\dots,N, \tag{2a}$$

$$\lim_{t\to+\infty}\sum_{j=1}^{N} a^c_{ij}(t) \le \bar{d}_i, \qquad i = 1,\dots N, \tag{2b}$$

that is, to synchronize the network topology and asymptotically limit to $\bar{d}_i$ the degree of node i in the control layer, for $i = 1,\dots,N$.

Here, we propose to attain this objective in a fully distributed fashion by dynamically updating the topology of the

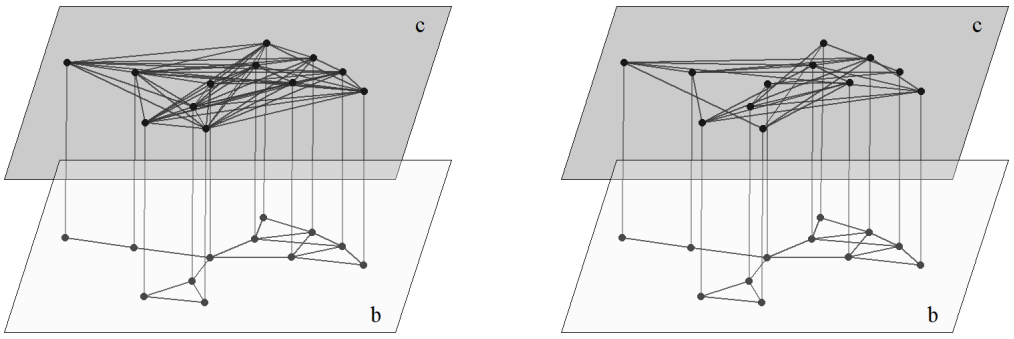

(a) (b)

FIG. 1. Schematic illustration of the proposed multilayer network model and examples of adaptation of the control layer in a network of Rössler oscillators, In panel (a), the control layer is obtained without limiting the resources, and setting the backbone and control gains as $k = 0.2$ and $q = 0.2$ respectively, and yields a control topology with $d_M = 10$ and $\langle d \rangle = 6.34$, whereas in panel (b) the resources are limited by setting $\bar{d} = 6$, thereby inducing a control layer with $d_M = 6$ and $\langle d \rangle = 5$. The figure shows the one-by-one node control which connects the control and backbone layers, identified by the letters c and b, respectively.

control layer according to a suitable modification of the classic edge snapping approach[19], whereby we associate a dynamical system to each pair of nodes in the network. Namely, for each pair ij, we introduce a state variable $\sigma_{ij} \in \mathbb{R}$, whose dynamics can be viewed as the motion of a mass in a double well potential, whereas the binary output of the pair ij will be the element $a^c_{ij}(t)$ of the adjacency matrix of the control layer, that is,

$$\ddot{\sigma}_{ij}(t) + \zeta \dot{\sigma}_{ij}(t) + \frac{\partial}{\partial \sigma_{ij}(t)} V(\sigma_{ij}(t)) = u_{ij}(t), \tag{3a}$$

$$a^c_{ij}(t) = \Theta(\sigma_{ij}(t) - 0.5), \tag{3b}$$

where ζ is the damping, $V(\sigma_{ij}) : \mathbb{R} \to \mathbb{R}$ is a double-well potential, $u_{ij}(t)$ is a time-varying input driving the edge dynamics, and Θ is the Heaviside function. In general, the potential $V(\sigma_{ij})$ is selected so that the homogeneous equation associated to (3a) has two locally stable equilibria in 0 and 1, and an unstable equilibrium in 0.5. As in standard edge snapping, we select

$$V(\sigma_{ij}) = b\sigma^2_{ij}(\sigma_{ij} - 1)^2, \tag{4}$$

where b is a positive scalar that modulates the height of the barrier between the two stable equilibria.

The main difference compared with the classic edge snapping stands in the selection of the input u_{ij}, which is tailored to avoid an excessive activation of edges in the control layer. Towards this goal, we start by defining, for all $i = 1, \ldots, N$, the variable

$$\delta_i(t) = \max\left(0, \sum_{j=1}^{N} a^c_{ij}(t) - \bar{d}_i\right), \tag{5}$$

which, when positive, is equal to the number of edges incident at i that exceed the asymptotic bound $\bar{d}_i$ on the degree of node i. Then, for each pair of nodes, we define $\delta_{ij}(t) = \delta_i(t) + \delta_j(t)$, which is positive if one of the two nodes has a number of edges exceeding the asymptotic bound ($\bar{d}_i$ or $\bar{d}_j$), that is, if it is using more resources than those allowed. Finally, we select the input as follows

$$u_{ij}(t) = \beta_1 g(e_{ij}(t)) - \beta_2 \delta_{ij}(t), \tag{6}$$

where $e_{ij}(t) = x_j(t) - x_i(t)$ and

$$g(e_{ij}(t)) = \left\| e_{ij}(t) \right\|, \tag{7}$$

In this way, the input $u_{ij}(t)$ takes into account two contributions. The first term, $\beta_1 g(e_{ij}(t))$, is a function of the local synchronization error between i and j and, as $\beta_1 > 0$, promotes the formation of a link between the two nodes if they are not synchronized. The second term, $-\beta_2 \delta_{ij}(t)$, is negative if one of the two nodes is using too many resources, and, in such case, as $\beta_2 > 0$, hampers the formation of the link. The two constants, β_1 and β_2, can be calibrated to weigh the importance of the two goals (2a) and (2b), respectively.

III. THEORETICAL ANALYSIS

In this section, we carry out a theoretical analysis on the local stability of the solution of model (1), (3) that are of interest considering the control goal stated in (2). Namely, we study the local stability of all the solutions corresponding to i) synchronous nodes, that is, $x_1 = \ldots = x_N = x_s$,[26] and ii) constant edge states with values $\overline{\sigma}_{ij}$ being either 0 or 1, and such that the degree bound $\sum_{j=1}^{N} a^c_{ij}(t) < \bar{d}_i$ is fulfilled for all i.

Toward this goal, let us indicate with $\delta x_i = x_i - x_s$ the transverse dynamics of the i-th unit, and let us define $\delta\sigma_{ij} = \sigma_{ij} - \overline{\sigma}_{ij}$ as the deviation of the edge state from the considered equilibrium $\overline{\sigma}_{ij}$. Furthermore, we can introduce $\delta x = \left[\delta x_1^{\mathrm{T}}, \ldots, \delta x_N^{\mathrm{T}}\right]^{\mathrm{T}}$, and the vectors $\delta\sigma$, and $\delta\dot{\sigma}$ stacking all the

$\delta\sigma_{ij}$'s and $\delta\dot{\sigma}_{ij}$'s, respectively. Linearizing the dynamics of $(\delta x, \delta\sigma)$ around the origin yields

$$\begin{aligned}\delta\dot{x} &= [\mathrm{I}_N \otimes \mathrm{Jf}(x_s) - k\mathrm{L}^{(b)} \otimes \mathrm{Jh}^{(\mathrm{b})}(x_s) - q\bar{\mathrm{L}}^{(c)} \otimes \mathrm{Jh}^{(\mathrm{c})}(x_s)]\delta x,\\ \delta\ddot{\sigma} &= -\zeta\delta\dot{\sigma} - 2b\delta\sigma,\end{aligned} \tag{8}$$

where we considered that the gradient of g is naught at the origin, and that δ_{ij} is constant (and equal to zero) around the origin. We remark that the assumption of a zero gradient of g at the origin is important to decouple the perturbations on the weights of the adaptive layer. This assumption is true for g in Eq. (7), and is therefore a design criterion for the updating law for the adaptive weights of the proposed approach. In Eq. (8) we denoted with $\mathrm{Jf}(x_s)$, $\mathrm{Jh}^{(\mathrm{b})}(x_s)$, and $\mathrm{Jh}^{(\mathrm{c})}(x_s)$ the Jacobians of the functions f, $h^{(b)}$, and $h^{(c)}$, respectively, evaluated at the synchronization manifold x_s, and with $\bar{\mathrm{L}}^{(c)}$ the constant Laplacian matrix corresponding to the reference equilibrium $\bar{\sigma}$ of the network edge state σ.

Notice that $\bar{\mathrm{L}}^{(c)}$ depends on the system evolution, and, hence, on the updating rule for the adaptive links, the system parameters, and initial conditions. In particular, while in classic edge snapping all possible topologies on N nodes are a feasible equilibrium configuration, here an admissible equilibrium topology should be such that δ_i is zero for all i, as implied by Eqs. (5)-(6), that is, the equilibrium degree $(\bar{\mathrm{L}}^{(c)})_{ii}$ of node i in the control layer should not exceed $\bar{\delta}_i$.

Since local node and edge dynamics in (8) are decoupled, we can study them separately. First, we notice that selecting positive values for ζ and b yields asymptotic stability of the linearized dynamics of $\delta\sigma$. We can then focus on the nodal dynamics around the synchronization manifold.

We start by observing that both $\mathrm{L}^{(b)}$ and $\bar{\mathrm{L}}^{(c)}$ are symmetric, positive semi-definite matrices, and thereby they share the eigenvalue $\lambda_1 = 0$, with associated eigenvector $v_1 = [1,\dots,1]^{\mathrm{T}}$ (for convenience we sort the eigenvalues in ascending order). In general, the other eigenvalues and eigenvectors of the two matrices are different, such that they cannot be simultaneously diagonalized. Let us then consider the matrix T containing the left eigenvectors of L^b and define the transformed variable $\xi = (\mathrm{T}^{-1} \otimes I_n)\delta x$. The dynamics of ξ can be written as

$$\begin{aligned}\dot{\xi} = [&\mathrm{I}_N \otimes \mathrm{Jf}(x_s) - k\mathrm{diag}\{\lambda_1(\mathrm{L}^{(b)}),\dots,\lambda_N(\mathrm{L}^{(b)})\} \otimes \mathrm{Jh}^{(\mathrm{b})}(x_s)\\ &- q\widehat{\mathrm{L}}^{(c)} \otimes \mathrm{Jh}^{(\mathrm{c})}(x_s)]\xi\end{aligned} \tag{9}$$

where $\widehat{\mathrm{L}}^{(c)} = \mathrm{T}^{-1}\bar{\mathrm{L}}^{(c)}\mathrm{T}$. Considering the spectral properties of matrices $\mathrm{L}^{(b)}$ and $\bar{\mathrm{L}}^{(c)}$, equation (9) can be recast as

$$\begin{aligned}\dot{\xi}_1 &= \mathrm{Jf}(x_s)\xi_1,\\ \dot{\xi}_j &= [\mathrm{Jf}(x_s) - k\lambda_j(\mathrm{L}^{(b)})\mathrm{Jh}^{(\mathrm{b})}(x_s)]\xi_j - q\sum_{l=2}^{N}\widehat{\mathrm{L}}^{(c)}_{jl}\mathrm{Jh}^{(\mathrm{c})}(x_s)\xi_l,\end{aligned} \tag{10}$$

for $j = 2,\dots,N$. Note that the first mode is associated to $\lambda_1 = 0$ and determines the stability of the motion along the synchronization manifold, whereas all the other modes are transverse to this manifold. When these transverse modes damp out, synchronization is stable, such that synchronization stability can be assessed by characterizing the largest Lyapunov exponent of the dynamics of $\xi_2,\dots\xi_N$.

When the coupling function is the same in the two layers, that is, $h^{(b)} = h^{(c)}$, a considerable simplification takes place. Under this assumption, in fact, we can define a new matrix $\mathrm{M} = k\mathrm{L}^{(b)} + q\bar{\mathrm{L}}^{(c)}$ and rewrite the first equation in (8) as

$$\delta\dot{x} = [\mathrm{I}_N \otimes \mathrm{Jf}(x_s) - \mathrm{M} \otimes \mathrm{Jh}^{(\mathrm{b})}(x_s)]\delta x. \tag{11}$$

If $k, q \geq 0$, since both $\mathrm{L}^{(b)}$ and $\bar{\mathrm{L}}^{(c)}$ are symmetric and positive semi-definite, then also matrix M is symmetric and positive semi-definite. Therefore, we can select the transformation T as the matrix whose columns are obtained by juxtaposing the left eigenvectors of M, and define again ξ as $\xi = (\mathrm{T}^{-1} \otimes I_m)\delta x$, thereby obtaining

$$\dot{\xi}_i = [\mathrm{Jf}(x_s) - \lambda_i(\mathrm{M})\mathrm{Jh}^{(\mathrm{b})}(x_s)]\xi_i, \tag{12}$$

where $\lambda_1(\mathrm{M}),\dots,\lambda_N(\mathrm{M})$ are the eigenvalues of M sorted in ascending order, that is, $0 = \lambda_1(\mathrm{M}) \leq \lambda_2(\mathrm{M}) \leq \dots \lambda_N(\mathrm{M})$. Local stability of the synchronization manifold requires that the transverse modes in (12), i.e., those for $i = 2,\dots,N$, damp out. This condition can be checked by calculating the maximum Lyapunov exponent associated to the generic equation

$$\dot{\eta} = [\mathrm{Jf}(x_s) - \alpha\mathrm{Jh}^{(\mathrm{b})}(x_s)]\eta$$

as a function of the parameter α, i.e., $\Lambda_{\max}(\alpha)$, and verifying that $\Lambda_{\max}(\alpha) < 0$ for all $\alpha \in \{\lambda_2(\mathrm{M}),\dots,\lambda_N(\mathrm{M})\}$.

The exact form of $\bar{\mathrm{L}}^{(c)}$ (and therefore of M) depends on the trajectory followed by the system (1)-(3) with input as in Eq. (6). As the input is a function only of the state variables, the system becomes autonomous, and the trajectory it follows only depends on the system equations, its parameters (including the bound on available resources), and its initial conditions. Since prior to the determination of the system trajectory $\bar{\mathrm{L}}^{(c)}$ is not known, the eigenvalues of M cannot be calculated and the condition $\lambda_{\max}(\alpha) < 0$ cannot be checked. Nonetheless, equation (12) can still provide some *a priori* insights on the stability of the synchronous manifold.

First, we point out that equation (12) has the exact form of the Master Stability Function (MSF) that characterizes the synchronization stability in single layer complex networks of coupled oscillators[27] and, therefore, the classification into different types of MSF can still be applied[28]. For the sake of simplicity, let us focus on systems with type II MSF, which represents the case of an unbounded stability region, whereby there exists a threshold value $\alpha \in \mathbb{R}$ such that $\Lambda_{\max}(\alpha) < 0$ for $\alpha \in [\alpha_1, \infty)$. For this class of systems, local stability of the synchronization manifold requires $\lambda_2(\mathrm{M}) > \alpha_1$. As M is the sum of two positive semidefinite matrices, we have that

$$\lambda_2(\mathrm{M}) \geq \max\{k\lambda_2(\mathrm{L}^{(b)}), q\lambda_2(\bar{\mathrm{L}}^{(c)})\} \geq q\lambda_2(\bar{\mathrm{L}}^{(c)}). \tag{13}$$

Suppose now that the backbone layer is not able to enforce local stability of the synchronization manifold, that is,

$\max\{k\lambda_2(\mathrm{L}^{(b)}), q\lambda_2(\mathrm{L}^{(c)})\} = q\lambda_2(\mathrm{L}^{(c)})$, such that the control problem is not trivial. A relevant degenerate case is when there is no backbone network at all, i.e., $k = 0$ and the topology is entirely dictated by the snapping dynamics; in that case $\lambda_2(\mathrm{M}) = q\lambda_2(\bar{\mathrm{L}}^{(c)})$. Furthermore, let us remind that, according to Eqs. (5)-(6), an admissible equilibrium configuration for the control layers is such that each node, say i, in the control layer does not overcome the threshold $\bar{d}_i$ introduced in (5). Therefore, in this case a necessary condition for synchronizability is the existence of an admissible equilibrium configuration, fulfilling the asymptotic constraint on the maximal number $\bar{d} = \max_i \bar{d}_i$ of edges incident at each node, such that $q \geq \alpha_1/\lambda_2(\bar{L}^{(c)})$. Reminding that the addition of a new edge can never decrease the Laplacian eigenvalues, and denoting with $\mathscr{L}_{\mathrm{reg}}(\bar{d})$ the class of static Laplacian matrices associated to $\bar{d}$-regular graphs (i.e. graphs such that all nodes have degree $\bar{d}$), we would then have that a necessary condition for synchronization is

$$q \geq \frac{\alpha_1}{\lambda_2\big(L_{\max}(\bar{d})\big)},$$

where

$$L_{\max}(\bar{d}) = \underset{L\in\mathscr{L}_{\mathrm{reg}}(\bar{d})}{\arg\max}\ \lambda_2(L).$$

Since an upper bound for the smallest non-zero eigenvalue of the Laplacian is its smallest degree, we then have $\lambda_2\big(L_{\max}(\bar{d}) \leq \bar{d}$, thereby obtaining

$$q \geq \frac{\alpha_1}{\bar{d}}. \tag{14}$$

When the control gain q is lower than $\underline{q} \triangleq \alpha_1/\bar{d}$, we can then conclude that synchronization with limited resources cannot be attained without either further increasing q, or relaxing the constraint on the maximal number of edges by modifying $\bar{d}_i$ in Eq. (5).

IV. ADAPTIVE NETWORKS OF COUPLED CHAOTIC OSCILLATORS

We first numerically test the effectiveness of our adaptive strategy on a network with $N = 12$ Rössler oscillators coupled only on their second state variable. Denoting with $[x_i\ y_i\ z_i]^{\mathrm{T}}$ the state vector of the i-th node, the network dynamics can be written as follows:

$$\begin{aligned}
\dot{x}_i &= -y_i - z_i,\\
\dot{y}_i &= x_i + a_R y_i + k\sum_{j=1}^{N} a^b_{ij}(y_j - y_i) + q\sum_{j=1}^{N} a^c_{ij}(t)(y_j - y_i),\\
\dot{z}_i &= b_R + z_i(x_i - c_R),
\end{aligned} \tag{15}$$

for $i = 1,\ldots,N$, with parameters $a_R = b_R = 0.2$ and $c_R = 9$, so that the uncoupled dynamics admit a chaotic attractor.

In our study, we have selected the backbone topology as in Fig. 1, and fixed the coupling coefficient to $k = 0.2$. With this choice, in the absence of control ($q = 0$), the network would not be synchronized. For the adaptive layer, we have selected $b = 5$ in (4), and $\beta_1 = 1$, $\beta_2 = 2.5$ in the input equation (6).

We have, therefore, evaluated whether the presence of the adaptive control layer can enforce synchronization in the network, by considering different choices for the parameters ruling the control layer, and in particular q and the resource constraints $\bar{d}_i$ in Eq. (5), here assumed equal for each node, that is, $\bar{d}_i = \bar{d}$ for all i. For different values of $\bar{d}$ (varied between 2 and 5 with step 1), we have simultaneously monitored the synchronization error E and the maximum degree d_M of the final configuration obtained in the control layer, i.e., after transient dynamics vanished out, as a function of the control gain q. The first parameter provides information on the level of synchronization reached by the network after adaptation and is defined as $E = \langle e(t)\rangle_T$ where

$$e(t) = \sqrt{\frac{1}{N(N-1)}\sum_{i=1}^{N}\sum_{j=1,j\neq i}^{N}\big\|e_{ij}\big\|} \tag{16}$$

and T is a sufficiently large time window, selected as $T = 200$s in our simulations; d_M is instead measured to verify whether the requirement on the resource constraint has been fulfilled or not.

As depicted in Fig. 2(a), we observe a decrease in the synchronization error E as the control gain q increases, up to a point around $q = 0.1$ such that, for larger q we always obtain values of E signalling that the network can reach synchronization. Below this threshold, synchronization can only be achieved if using more resources, that is, for larger values of $\bar{d}$. This is also confirmed when looking at panel (b): for low values of the gain, the available resources are not sufficient, and the snapping mechanism tries to activate more edges. Nonetheless, synchronization cannot be stably enforced, since the violation of the asymptotic constraint on the resources, with some δ_i-s in (5) being positive, pushes towards edge deactivation.

When comparing our modified adaptive law with the classic edge-snapping approach, which operates with unbounded resources, we observe that the latter activates a relatively high number of links, which are not strictly required for synchronizing the network, as illustrated in Fig. 3 where we plot both the maximum degree d_M and average degree, $\langle d\rangle$ of the control layer as a function of q. In the classic edge snapping, there often are nodes that activate all possible links, whereby we observe $d_M = N - 1$, see panel (a). This happens since the initial conditions are randomly selected, and some nodes have a high initial synchronization error, triggering the activation of all possible connections. The new adaptation mechanism, instead, explicitly takes into account in the input (5)-(6) the need of not saturating the available resources, thereby significantly reducing the average number of activated links, see panel (b).

To better characterize the system behavior with respect to its main parameters, we have also studied the behavior for two selected values of $\bar{d}$ (3 and 6, respectively) by varying the control gain q between 0 and 0.2 with step 0.01, and the coupling strength k on the backbone layer between 0 and 1 with step 0.05, and then registering the synchronization error. The color

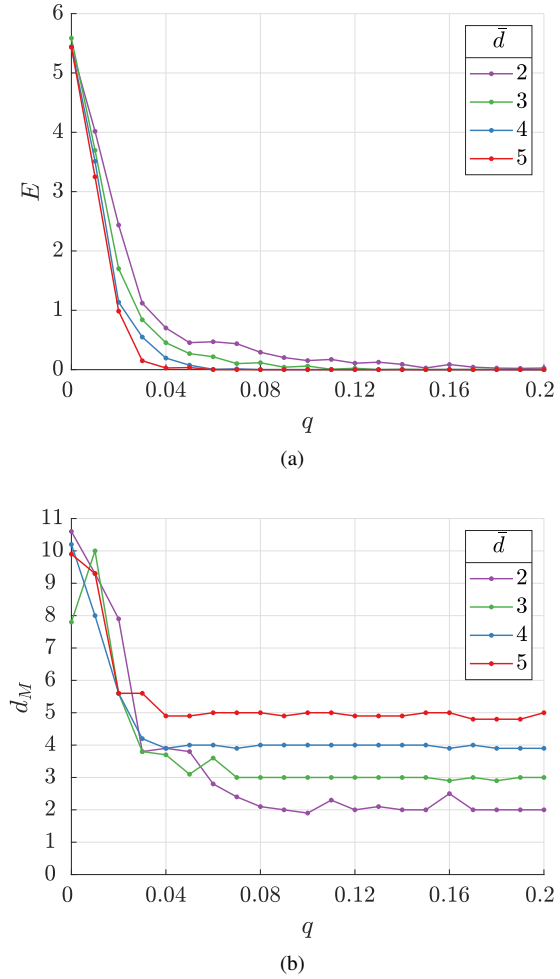

FIG. 2. Average synchronization error E (a) and maximum degree d_M (b) as a function of the control gain q the network of $N = 12$ depicted in Fig. 1 for different values of $\bar{d}$. The coupling strength of the backbone layer is set $k = 0.2$, and results are averaged over 10 runs for each value of q.

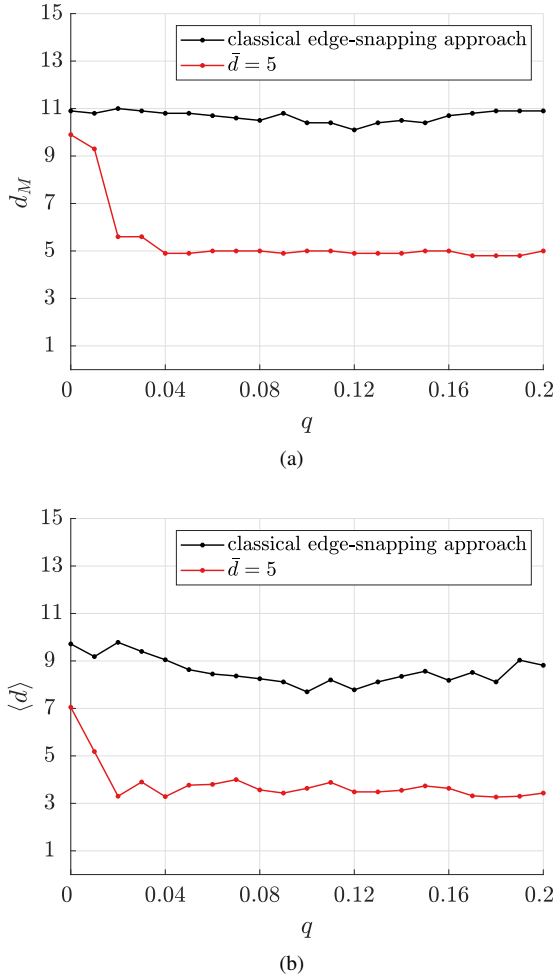

FIG. 3. Maximum degree d_m (a) and average degree $\langle d \rangle$ (b) of the control layer as a function of the control gain q for the classic edge snapping mechanism (without resource constraints) and for the proposed adaptive mechanism with $\bar{d} = 5$.

maps in Fig. 4 show that, for both values of $\bar{d}$, synchronization is attained in a wide region of the parameter space, where coupling coefficients k and q are sufficiently high. In addition, we observe a synergy between the two layers, whereby increasing k reduces the minimum value of q needed to achieve synchronization decreases, and viceversa.

In Eqs. (15) the same coupling function is used in the two layers, i.e., $h^{(b)} = h^{(c)}$, such that the stability of synchronization can be studied with Eq. (12). This system has a MSF of type II with $\alpha_1 = 0.157$ and, for the backbone network, the smallest non-zero eigenvalue of the Laplacian matrix is $\lambda_2 = 0.273$. Hence, when $q = 0$, synchronization requires that $k > \alpha_1/\lambda_2 = 0.575$. On the contrary, when $k = 0$, the necessary condition (14) gives, for $\bar{d} = 6$, $q > 0.023$ and, for $\bar{d} = 3$, $q > 0.052$, in line with the colormap in Fig. 4(b).

Finally, another interesting aspect to study is the effect of the new adaptive law on the emergent topology when there is no pristine structure of interconnections at all, namely $\mathrm{A}^b = 0$. This corresponds to consider a single-layer that is adaptive, as in the original edge-snapping formulation[19]. We have considered an ensemble of $N = 100$ Rössler oscillators, starting from an initial condition with $\sigma_{ij}(0) = 0$ for any i and j, that is, from a configuration where all adaptive links are set to zero. We evolved this structure with the adaptive law introduced in Sec. II B in a total of 100 runs, for both the case of unlimited resourced and of limited resources so that $\bar{d}_i = \bar{d} = 8$ for all i in (5), and we obtained the average degree distributions shown in Fig. 5. The notable effect of including a bound on the available resources is to shift the mean value of the degree distribution and to truncate it. In fact, while, in the case of unlimited resources a Poissonian-like degree distribution is obtained, when, on the contrary, resources are limited, the resulting degree distribution is peaked at $d = 5$ and truncated at the bound value $d = \bar{d}$.

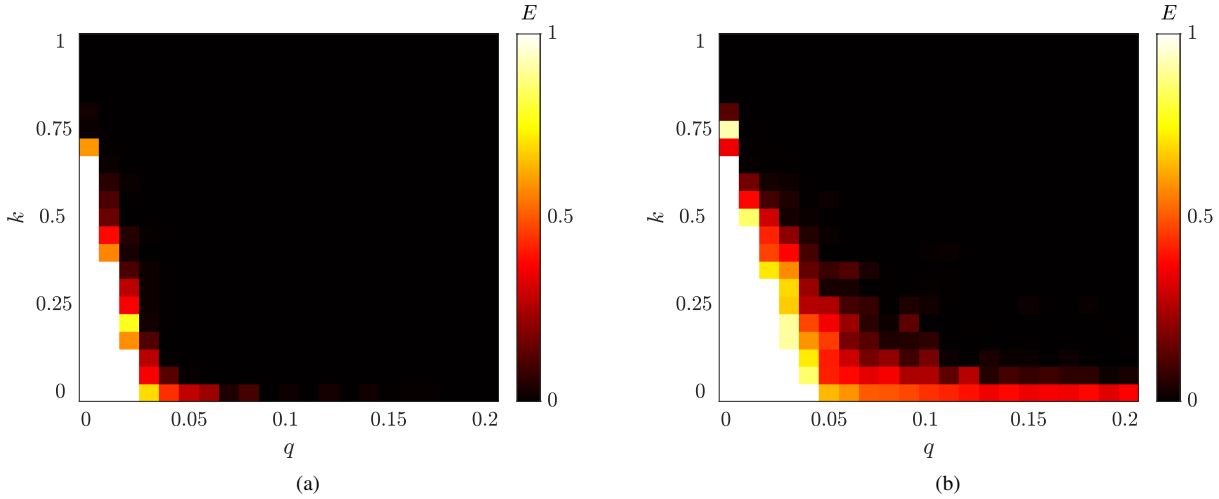

FIG. 4. Color map of the synchronization error E as a function of the control gain q and the coupling strength k of the backbone layer for a system of coupled Rössler oscillators, for $\bar{d} = 6$ (a) and $\bar{d} = 3$ (b), respectively (all values of E larger than 1 are depicted in white). The backbone network is shown in Fig. 1. Results are averaged over 10 runs for each pair (q,k).

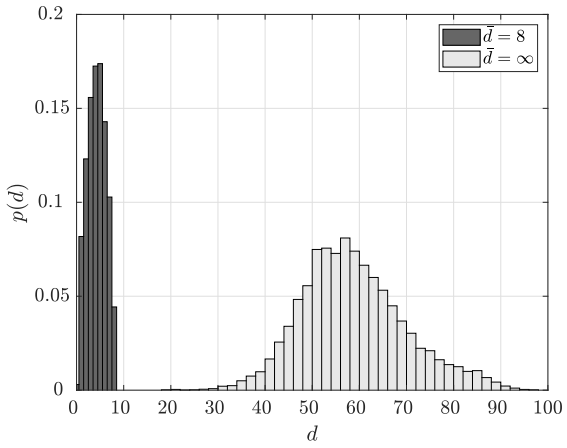

FIG. 5. Degree distribution of the control layer when there is no backbone network, namely $A^b = 0$, for a system of $N = 100$ Rössler oscillators, with ($\bar{d} = 8$) or without ($\bar{d} = \infty$) limited resources. The control gain is set as $q = 2.5$, while all the other parameters of the updating law are as in the text. Results are averaged over 100 runs.

V. APPLICATION OF THE ADAPTIVE LAW TO THE ITALIAN POWER GRID MODEL

In this section, we study the use of the adaptive law (3) to control synchronization in a model of the Italian power grid, in order to show that our approach does not apply only to the canonical network model in Eq. (1), but also to a model that captures more realistic complexities. In fact, the model that we will consider in this section differs from Eq. (1) as the system units are no more identical. In addition, the sought synchronization property for the power grid model is phase synchronization, rather than complete synchronization. For this reason, the theoretical analysis presented in Sec. III cannot be applied, but we will show that still the control law we have proposed is effective as the key mechanisms of the adaptive law at work do not depend on the specific form of system to which they are applied. Our analysis is framed in the context of power grids, as for these networks the ability to reconfigure the links in the presence of failures is paramount. In the following, we will therefore consider a model of the Italian power grid that includes failure mechanisms for the network links, and test how the control layer reacts to failures at selected lines.

A. Power grid model

We consider a power grid equipped with a control cyber-layer[29] with limited resources, that is, under constraints on the number of edges that can be activated. The model we consider assumes that each of the N nodes of the power system is described by a swing equation according to the synchronous machine representation of the power grid[30,31]. Each node also receives a control input generated in a second layer, which works in parallel with the physical one and with a control action that is proportional to the node frequency differences. Omitting the explicit dependence on time for brevity, the dynamics of the resulting system is described by the following equations:

$$\frac{d\theta_i}{dt} = \omega_i \tag{17}$$
$$I_i \frac{d\omega_i}{dt} = P_i - \gamma_i \omega_i + \sum_{j=1}^{N} a^b_{ij} \sin(\theta_j - \theta_i) + k_c \sum_{j=1}^{N} a^c_{ij} (\omega_j - \omega_i)$$

for $i = 1,\ldots,N$, where θ_i represents the voltage phase angle and ω_i the angular velocity of the i-th synchronous machine, expressed in a reference frame rotating with angular speed $\Omega = 2\pi f$, with f being 50 Hz or 60 Hz, depending on the ge-

ographical area under study; I_i and γ_i are the constant inertia and damping coefficient associated to the i-th synchronous machine of the power system; the power P_i is a positive constant parameter for the nodes that inject the power into the system (generators), whereas it is negative for the nodes that absorb the power from the system (loads); the coefficients a^b_{ij} are the elements of a weighted adjacency matrix describing the operative lines of the power grid topology, and are related to the electrical quantities characterizing the nodes by the relationship $a^b_{ij} = B_{ij}V_iV_j$, where B_{ij} is the susceptance between nodes i and j, and V_i and V_j are the voltage amplitudes at nodes i and j, respectively. The coefficients a^c_{ij} are the elements of the adjacency matrix (assumed undirected and unweighted) associated to the control layer, which in Ref.[29] have been considered fixed in time and with a topology equal to the physical layer. Here, on the contrary, we let these coefficients evolve in time according to the adaptation law (3)-(6).

The model also takes into account dynamical failures of the lines by considering the flow associated at each edge (i,j), i.e., $F_{ij}(t) = a^b_{ij}\sin(\theta_j(t) - \theta_i(t))$, and checking whether it exceeds the maximum capacity of the line. Following Ref.[32], the maximum line capacity is defined as $C_{ij} = \alpha a^b_{ij}$, and $\alpha \in [0,1]$ is a tunable parameter. Therefore, we say that line line (i,j) is in overload when

$$|F_{ij}(t)| > C_{ij} = \alpha a^b_{ij} \tag{18}$$

If this condition is met at some time $t = t_f$, to avoid overheating due to ohmic losses the line is shutdown, by setting in the model $a^b_{ij} = 0$ for $t > t_f$.

B. Control objective

In our analysis, we consider a fault due to some exogenous event, located at a line (i',j'). This fault generates a transient where the power grid operates out of synchrony, and eventually induces a cascade of failures in other lines where the flow overcomes the maximum capacity[32,33]. At the same time, the loss of synchrony triggers the adaptive mechanisms embedded in the links of the control layer and activates the control inputs, $u_i = k_c\sum_{j=1}^N a^c_{ij}(\omega_j - \omega_i)$, that attempt to restore synchrony in the network, thus limiting the flows in the lines. The effectiveness of such a control strategy in preventing the propagation of the faults into a cascade of successive failures has been demonstrated over a static topology, copy of the physical layer, in Ref.[29]. Here, we show that the topology of the control layer can be adaptively selected in a decentralized fashion to avoid the onset of cascading failures and maintain synchronization.

C. The Italian high-voltage power grid

Here, we tailor the power grid model (17) to the case of the Italian high-voltage (380kV) power grid[30,34–38]. This network is assumed homogeneous and undirected, that is, $a^b_{ij} = a^b_{ji} = k$ if there is a link between i and j, and $a^b_{ij} = a^b_{ji} = 0$ otherwise.

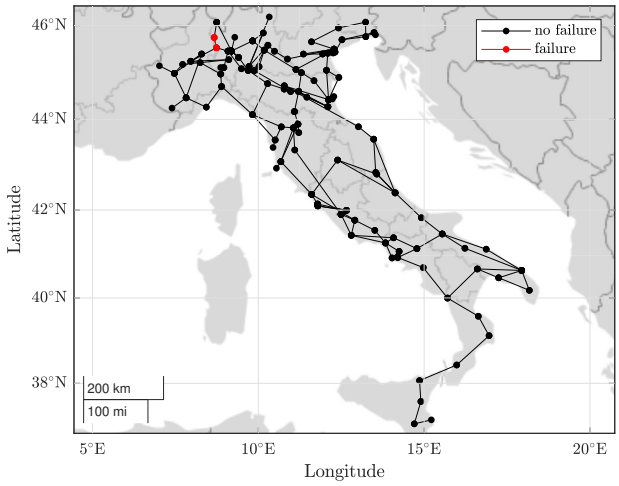

FIG. 6. Schematic of the Italian high-voltage (380kV) power grid.

The network consists of $N = 127$ nodes (34 generators and 93 loads) and $L = 171$ links (Fig. 6). Following Ref.[29], the parameters of the swing equations modeling the dynamics of the power grid have been set as $\gamma = 0.1$, $\alpha = 0.6$, $k = 15$, $P_i = -1$ for the load nodes, and $P_i = 2.735$ for the generation nodes, such that the network is balanced, i.e., $\sum_{i=1}^N P_i = 0$. With this parameter selection, the network is synchronized in the absence of faults. In the adaptive layer, as the controller aims at synchronizing all the frequencies in the grid, we have considered $g(e_{ij})$ as function solely of the frequency difference between nodes i and j, that is, we have set $g(e_{ij}) = |\omega_i - \omega_j|$. As in Sec. II, the parameters of the potential function (4) have been selected as $\zeta = 1$, and $b = 5$, the control gains has been chosen as $q = 15$, whereas the parameters of the control law (3) have been set to $\beta_1 = 20$, and $\beta_2 = 2.5$.

D. Numerical results

First, we have analyzed the behavior of the power grid model in the absence of control ($q = 0$) in the following setting: the grid initially operates in synchrony, then, at time $t = t_f = 1$ s, a fault occurs in a single line of the network, possibly triggering a cascading failure. We have numerically integrated Eqs. (17) for a total time $T = 20$ s, while monitoring the flows to check whether at some point in time they overcame the line maximum capacity (Eq. (18)), thereby leading to the failure of the line. This analysis reveals that there are 16 critical lines (i.e., lines that effectively trigger a cascading failure). For these specific lines, we have then studied the effect of the adaptive control layer in restoring synchronization and preventing the cascading failures.

For the purpose of illustration, let us first focus on the failure of the line $(10,16)$ that, in the absence of control, triggers a cascading failure of five other lines[29]. Without any constraint on the resources available at each node, the evolution of the adaptive layer yields a structure with $L_c = 251$ links, with an average degree of $\langle d\rangle = 3.95$, see Fig. 7 (a). How-

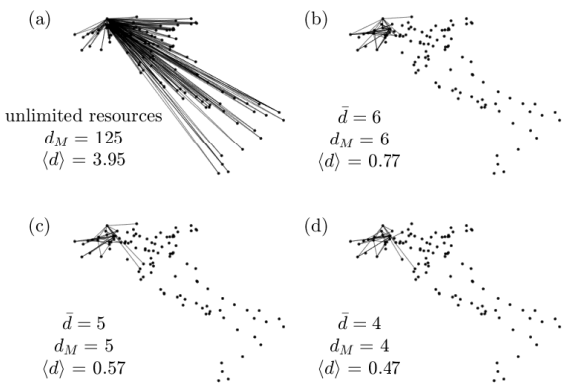

FIG. 7. Control layer of the Italian high-voltage power grid obtained after failure of the line (10,16) (shown in red in Fig. 6) in the absence of constraints on the available resources (a), and when $\bar{d}$ is equal to 6 (b), 5 (c), and 4 (d), respectively.

ever, the large majority of these links are not strictly necessary for control, as the use of adaptation rule (3)-(6) with finite $\bar{d}_i$ demonstrates. Indeed, in Fig. 7, panels (b-d), we show that it is possible to successfully control the power grid, preventing the cascading failures and recovering frequency synchronization after the initial fault, with a much lower number of links and corresponding average degree. Specifically, we obtain $L_c = 49$ ($\langle d \rangle = 0.77$) for $\bar{d}_i = 6$, $L_c = 36$ ($\langle d \rangle = 0.57$) for $\bar{d}_i = 5$, and $L_c = 30$ ($\langle d \rangle = 0.47$) for $\bar{d}_i = 4$.

Let us now illustrate the results of the analysis for each of the 16 lines identified as critical since they trigger cascading failures in the absence of the control layer. Table I reports, for each line, the differentiated use of resources in four different cases: no upper bound on the resources available at each node as in the classic edge snapping mechanism, and limited resources with $\bar{d}$ equal to 6, 5, or 4, respectively. For each case, the maximum node degree d_M and the average node degree $\langle d \rangle$ in the control layer have been calculated. In all the cases, the control input was able to restore synchronization, at the same time preventing the failure of other lines of the grid. Moreover, we found that, in all cases where the resources were constrained, d_M was always equal to $\bar{d}$, whereby the resource constraints were always fulfilled. Furthermore, a closer look at the parameter $\langle d \rangle$, quantifying how many links are activated in the control layer ($L_c = \langle d \rangle N/2$), shows that the average degree is typically much lower than the constraint d_M, so that additional links are only added where they are actually needed. In addition, this parameter allowed to emphasize that some faults require the activation of more nodes compared to other faults. For instance, considering a resource constraint $\bar{d} = 4$, we find that recovering from an initial fault located in the line $(59,61)$ requires a larger number of links $L_c = 67$ than from a fault in $(21,23)$, where $L_c = 28$. Although beyond the scope of this work, it would be interesting to investigate whether and how $\langle d \rangle$ or L_c can be related to the topological properties of the links where the initial fault occurs.

TABLE I. Characteristic parameters of the adaptive control layer of the Italian high-voltage (380kV) power grid model, for different locations of initial fault and assumptions on the available resources at each node.

Fault line	$\bar{d}$	d_M	$\langle d \rangle$	Fault line	$\bar{d}$	d_M	$\langle d \rangle$
(10,16)	∞	125	3.95	(15,16)	∞	124	7.69
	6	6	0.77		6	6	0.38
	5	5	0.57		5	5	0.35
	4	4	0.47		4	4	0.27
(15,17)	∞	123	7.59	(20,21)	∞	124	2.27
	6	6	0.43		6	6	0.54
	5	5	0.36		5	5	0.68
	4	4	0.28		4	4	0.52
(21,22)	∞	117	4.06	(21,23)	∞	125	4.00
	6	6	1.18		6	6	0.74
	5	5	0.98		5	5	0.57
	4	4	0.79		4	4	0.44
(27,59)	∞	122	5.76	(33,35)	∞	126	5.81
	6	6	0.83		6	6	0.47
	5	5	0.85		5	5	0.46
	4	4	0.69		4	4	0.46
(36,38)	∞	123	7.67	(59,60)	∞	123	3.97
	6	6	0.47		6	6	1.78
	5	5	0.47		5	5	1.07
	4	4	0.36		4	4	1.13
(59,61)	∞	124	7.67	(64,78)	∞	123	4.27
	6	6	1.42		6	6	1.37
	5	5	1.13		5	5	0.93
	4	4	1.06		4	4	1.09
(75,88)	∞	121	4.25	(76,79)	∞	122	4.24
	6	6	1.15		6	6	1.37
	5	5	1.54		5	5	1.23
	4	4	1.09		4	4	1.06
(79,80)	∞	123	5.78	(86,88)	∞	123	5.81
	6	6	0.74		6	6	0.69
	5	5	0.85		5	5	0.68
	4	4	1.02		4	4	0.60

VI. CONCLUSIONS

In this work, we have introduced a multilayer control protocol for synchronization of coupled dynamical systems under the constraint of limited resources available at each node. The control is structured as a second layer acting in parallel to a set of links that are fixed in time and constitute the backbone of the network. The interactions in the control layer are adaptive so that they can be activated or removed as a function of the level of synchronization and the available resources. The adaptive mechanism we have proposed introduces a discontinuous output function that, together with a modified input to the snapping dynamics, allow to extend the classic edge snapping algorithm, and incorporate constraints on the degree of each node in the network. As the classical edge snapping, our approach provides a fully distributed technique able to

evolve the structure of interconnections, different from other methods[7,10–12] that only operate on the coupling gains of a pre-existing network. However, at variance with the classical edge snapping our approach allows to obtain synchronization with a much smaller average degree, thus overcoming an important limitation of the previous technique.

The approach has been demonstrated and applied to a network of coupled Rössler oscillators and then extended to a more general setting exemplified with a model of the Italian high-voltage power grid. For the network of Rössler oscillators, we have shown that suitable values of the coupling coefficient of the control layer guarantees the stability of the synchronous solution, while at the same time satisfying the constraint on the limited resources. In addition, the two layers act in synergy so that a lower control gain is required as the coupling strength in the backbone network increases. We have then considered a model of the Italian high-voltage power grid, based on the swing equations and incorporating a mechanism to account for link failures induced by the dynamical evolution of the grid. We have applied the key mechanism of our control law to this system as well, in order to test its robustness to a more general setting that deviates from the assumptions underlying the canonical model. The adaptive control strategy has been shown able to guarantee synchronization and prevent cascading failures, even in the case of limited resources.

There are several directions along which our work can be expanded. First, in all the illustrated numerical results, we have set the same upper bound for all node degrees. However, the strategy is more general and different values for each node can be considered, thus differentiating the amount of resources available at the various nodes. A further straightforward generalization is to restrict the set of links that can be adapted in the control layer to incorporate in the model further constraints on the topology of the evolved network. Finally, in all scenarios where the number of controlled nodes may be relevant, it should be possible to apply the proposed adaptive control law only to a subset of the nodes of the backbone structure.

ACKNOWLEDGMENTS

This work was supported by the Italian Ministry for Research and Education (MIUR) through Research Program PRIN 2017 under Grant 2017CWMF93, project "Advanced Network Control of Future Smart Grids - VECTORS".

[1]D. Ghosh, M. Frasca, A. Rizzo, S. Majhi, S. Rakshit, K. Alfaro-Bittner, and S. Boccaletti, "The synchronized dynamics of time-varying networks," *Physics Reports*, vol. 949, pp. 1–63, 2022.

[2]F. Della Rossa and P. De Lellis, "Synchronization and pinning control of stochastic coevolving networks," *Annual Reviews in Control*, vol. 54, pp. 147–160, 2022.

[3]D. D. Šiljak, "On stability of large-scale systems under structural perturbations," *IFAC Proceedings Volumes*, vol. 6, no. 2, pp. 440–443, 1973.

[4]D. Šiljak, "Dynamic graphs," *Nonlinear Analysis: Hybrid Systems*, vol. 2, no. 2, pp. 544–567, 2008.

[5]J. H. Holland, *Adaptation in natural and artificial systems: an introductory analysis with applications to biology, control, and artificial intelligence*. MIT press, 1992.

[6]T. E. Gorochowski, M. D. Bernardo, and C. S. Grierson, "Evolving dynamical networks: a formalism for describing complex systems," *Complexity*, vol. 17, no. 3, pp. 18–25, 2012.

[7]P. DeLellis, M. Di Bernardo, T. E. Gorochowski, and G. Russo, "Synchronization and control of complex networks via contraction, adaptation and evolution," *IEEE Circuits and Systems Magazine*, vol. 10, no. 3, pp. 64–82, 2010.

[8]F. G. Hillary and J. H. Grafman, "Injured brains and adaptive networks: the benefits and costs of hyperconnectivity," *Trends in Cognitive Sciences*, vol. 21, no. 5, pp. 385–401, 2017.

[9]H. Sayama, I. Pestov, J. Schmidt, B. J. Bush, C. Wong, J. Yamanoi, and T. Gross, "Modeling complex systems with adaptive networks," *Computers & Mathematics with Applications*, vol. 65, no. 10, pp. 1645–1664, 2013.

[10]C. Zhou and J. Kurths, "Dynamical weights and enhanced synchronization in adaptive complex networks," *Physical Review Letters*, vol. 96, no. 16, p. 164102, 2006.

[11]T. Chen and X. Liu, "Network synchronization with an adaptive coupling strength," *arXiv preprint math/0610580*, 2006.

[12]P. De Lellis, M. Di Bernardo, F. Sorrentino, and A. Tierno, "Adaptive synchronization of complex networks," *International Journal of Computer Mathematics*, vol. 85, no. 8, pp. 1189–1218, 2008.

[13]T. Aoki and T. Aoyagi, "Co-evolution of phases and connection strengths in a network of phase oscillators," *Physical Review Letters*, vol. 102, no. 3, p. 034101, 2009.

[14]S. Assenza, R. Gutiérrez, J. Gómez-Gardenes, V. Latora, and S. Boccaletti, "Emergence of structural patterns out of synchronization in networks with competitive interactions," *Scientific Reports*, vol. 1, p. 99, 2011.

[15]R. Gutiérrez, A. Amann, S. Assenza, J. Gómez-Gardenes, V. Latora, and S. Boccaletti, "Emerging meso-and macroscales from synchronization of adaptive networks," *Physical Review Letters*, vol. 107, no. 23, p. 234103, 2011.

[16]E. Estrada, "Network robustness to targeted attacks. the interplay of expansibility and degree distribution," *The European Physical Journal B-Condensed Matter and Complex Systems*, vol. 52, no. 4, pp. 563–574, 2006.

[17]P. DeLellis, A. DiMeglio, F. Garofalo, and F. Lo Iudice, "The evolving cobweb of relations among partially rational investors," *PLoS One*, vol. 12, no. 2, p. e0171891, 2017.

[18]P. DeLellis, M. di Bernardo, and M. Porfiri, "Pinning control of complex networks via edge snapping," *Chaos: An Interdisciplinary Journal of Nonlinear Science*, vol. 21, no. 3, p. 033119, 2011.

[19]P. DeLellis, F. Garofalo, M. Porfiri *et al.*, "Evolution of complex networks via edge snapping," *IEEE Transactions on Circuits and Systems I: Regular Papers*, vol. 57, no. 8, pp. 2132–2143, 2010.

[20]D. A. Burbano and M. di Bernardo, "Distributed PID control for consensus of homogeneous and heterogeneous networks," *IEEE Transactions on Control of Network Systems*, vol. 2, no. 2, pp. 154–163, 2014.

[21]——, "Multiplex PI control for consensus in networks of heterogeneous linear agents," *Automatica*, vol. 67, pp. 310–320, 2016.

[22]L. V. Gambuzza, M. Frasca, and J. Gomez-Gardenes, "Intra-layer synchronization in multiplex networks," *EPL (Europhysics Letters)*, vol. 110, no. 2, p. 20010, 2015.

[23]C. I. Del Genio, J. Gómez-Gardeñes, I. Bonamassa, and S. Boccaletti, "Synchronization in networks with multiple interaction layers," *Science Advances*, vol. 2, no. 11, p. e1601679, 2016.

[24]I. Belykh, D. Carter, and R. Jeter, "Synchronization in multilayer networks: When good links go bad," *SIAM Journal on Applied Dynamical Systems*, vol. 18, no. 4, pp. 2267–2302, 2019.

[25]L. Tang, X. Wu, J. Lü, J.-a. Lu, and R. M. D'Souza, "Master stability functions for complete, intralayer, and interlayer synchronization in multiplex networks of coupled rössler oscillators," *Physical Review E*, vol. 99, no. 1, p. 012304, 2019.

[26]Note that the invariance of the synchronization manifold is guaranteed by the diffusive nature of the coupling protocols in (1).

[27]L. M. Pecora and T. L. Carroll, "Master stability functions for synchronized coupled systems," *Physical Review Letters*, vol. 80, no. 10, p. 2109, 1998.

[28]S. Boccaletti, V. Latora, Y. Moreno, M. Chavez, and D.-U. Hwang, "Complex networks: Structure and dynamics," *Physics Reports*, vol. 424, no. 4-5, pp. 175–308, 2006.

[29]M. Frasca and L. V. Gambuzza, "Control of cascading failures in dynamical models of power grids," *Chaos, Solitons & Fractals*, vol. 153, p. 111460,

2021.
[30]G. Filatrella, A. H. Nielsen, and N. F. Pedersen, "Analysis of a power grid using a kuramoto-like model," *The European Physical Journal B*, vol. 61, no. 4, pp. 485–491, 2008.
[31]T. Nishikawa and A. E. Motter, "Comparative analysis of existing models for power-grid synchronization," *New Journal of Physics*, vol. 17, no. 1, p. 015012, 2015.
[32]B. Schäfer, D. Witthaut, M. Timme, and V. Latora, "Dynamically induced cascading failures in power grids," *Nature Communications*, vol. 9, no. 1, pp. 1–13, 2018.
[33]Y. Yang and A. E. Motter, "Cascading failures as continuous phase-space transitions," *Physical review letters*, vol. 119, no. 24, p. 248302, 2017.
[34]"GENI—Global Energy Network Institute, Map of Italian electricity grid," https://www.geni.org/globalenergy/library/national_energy_grid/italy/italiannationalelectricitygrid.shtml, [Online; accessed 21-December-2020].
[35]V. Rosato, S. Bologna, and F. Tiriticco, "Topological properties of high-voltage electrical transmission networks," *Electric Power Systems Research*, vol. 77, no. 2, pp. 99–105, 2007.
[36]L. Fortuna, M. Frasca, and A. Sarra Fiore, "A network of oscillators emulating the italian high-voltage power grid," *International Journal of Modern Physics B*, vol. 26, no. 25, p. 1246011, 2012.
[37]L. Tumash, S. Olmi, and E. Schöll, "Stability and control of power grids with diluted network topology," *Chaos: An Interdisciplinary Journal of Nonlinear Science*, vol. 29, no. 12, p. 123105, 2019.
[38]C. H. Totz, S. Olmi, and E. Schöll, "Control of synchronization in two-layer power grids," *Physical Review E*, vol. 102, no. 2, p. 022311, 2020.